Controllability Analysis of an Inverter Fed Induction Machine

Henrik Mosskull
Bombardier Transportation, SE-721 73 Västerås, Sweden
S3, Automatic Control, KTH, SE-100 44 Stockholm, Sweden

Abstract: A controllability analysis of an induction machine fed by a voltage source inverter is performed to gain understanding of fundamental properties of the process from a control point of view. For example the effects of input constraints on reference tracking as well as disturbance rejection are considered and some of the results are verified through simulations.

I INTRODUCTION

Due to their rugged mechanical construction, induction machines are commonly used in industrial and traction applications and several methods to control the torque and flux of such motors have appeared in the literature, see e.g. [1] and [2]. When evaluating different control methods, it is valuable to know the limits of performance. What actually set the bounds on the achievable performance are fundamental properties of the process itself as well as constraints on the inputs. Uncertainty of the process, including actuators, also restrict performance as robustness and performance are usually conflicting requirements. These issues are rarely addressed in connection to discussions of torque control algorithms. This paper however performs a controllability analysis as described in [3] of the induction motor fed by a voltage source inverter. Some similar results are presented in [4]. As the induction motor is a non-linear system it is linearized and examined at a number of operating points. Data for the motor examined in this work are given in the appendix.

II INDUCTION MACHINE DRIVE

Modern drives often use voltage source inverters to feed the induction motors, as shown in Figure 1. The input filter is used to suppress disturbances on the line voltage, $E(t)$, caused by the inverter. The coupling vector, $k(t)$, determines the state of each converter phase as a function of time and $\omega_m(t)$ is the mechanical rotor speed. Although the coupling vector contains a lot of high frequency components, only the fundamental will be considered in this work. Hence, the inverter is simply modeled by the following complex-valued *space vector* equation

$$u_s^s(t) = k^s(t)U_d(t) \approx \frac{u^s(t)}{U_d^*} \cdot U_d(t). \qquad (1)$$

Here space vectors are indicated by superscripts s and $u^s(t)$ represents the requested stator voltage, with magnitude and angle denoted $m_u(t)$ and $\chi_u(t)$ respectively. Furthermore, $U_d(t)$ and U_d^* denote the actual and nominal DC-link voltages of the inverter.

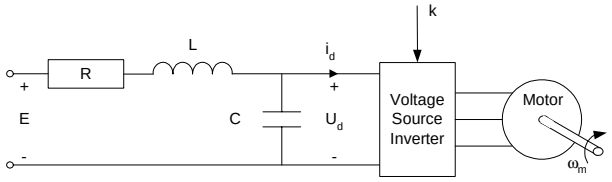

Figure 1: Induction machine drive.

The induction machine can be described by [4]

$$\dot{\psi}_\mu^s(t) = -R_s\left(\frac{1}{L_\mu}+\frac{1}{L_\sigma}\right)\psi_\mu^s(t) + \frac{R_s}{L_\sigma}\psi_r^s(t) + u_s^s(t) \qquad (2)$$

$$\dot{\psi}_r^s(t) = \frac{R_r}{L_\sigma}\psi_\mu^s(t) + \left(jp\omega_m(t) - \frac{R_r}{L_\sigma}\right)\psi_r^s(t) \qquad (3)$$

Here $\psi_\mu^s(t)$ and $\psi_r^s(t)$ represent the stator and rotor fluxes and p the number of pole pairs of the induction motor. R_s and R_r stand for the resistance in the stator and rotor windings and the machine inductances are denoted L_μ and L_σ. This representation, where all leakage inductance is put in the rotor mesh, is called the Γ-model. Using a polar notation with magnitudes and angles for the fluxes, i.e.

$$\psi_\mu^s(t) = m_\mu(t)e^{j\chi_\mu(t)}, \quad \psi_r^s(t) = m_r(t)e^{j\chi_r(t)}, \qquad (4)$$

then the electrical torque can be expressed as [4]

$$T = \frac{3}{2}\frac{p}{L_\sigma}m_\mu(t)m_r(t)\sin\left(\chi_\mu(t) - \chi_r(t)\right). \qquad (5)$$

III INPUT CONSTRAINTS

The maximum fundamental stator voltage magnitude depends on the inverter DC-link voltage, U_d, see e.g. [6]. As a matter of fact, the magnitude of the requested stator voltage is restricted to

$$m_u(t) = \left|u_s^s(t)\right| \le \frac{2}{\pi}U_d. \qquad (6)$$

Additionally, the frequency of the generated voltage should be restricted to prevent the steady state

slip frequency, ω_{slip}^*, from exceeding the pull-out slip frequency [6] which produces a lot of current. That is

$$\left|\omega_{slip}^*\right| = \left|\omega_u^* - p\omega_m^*\right| \le \frac{1}{T_\sigma} \tag{7}$$

where the *stator frequency*, $\omega_u(t)$, is the time derivative of $\chi_u(t)$ and $T_\sigma = L_\sigma/R_r$ is the rotor stray time constant.

IV LINEAR PROCESS MODEL

The inverter fed induction machine is described by equations (1), (2), (3) and (5). Inputs are the three stator voltages, represented by the magnitude and frequency of the stator voltage space vector $u^s(t)$, and outputs are the control variables torque and, in this case, the stator flux magnitude. The DC-link voltage and the mechanical rotor speed also affect the plant and are considered as disturbances. To obtain a linear model of the process, the equations are rewritten in the following way

$$\dot{m}_\mu = -R_s\left(\frac{1}{L_\mu}+\frac{1}{L_\sigma}\right)m_\mu + \frac{R_s}{L_\sigma}m_r\cos\delta + \frac{m_u U_d}{U_d^*}\cos\delta_{u\mu} \tag{8}$$

$$\dot{m}_r = \frac{1}{T_\sigma}m_\mu\cos\delta - \frac{1}{T_\sigma}m_r \tag{9}$$

$$\dot{\delta}_{u\mu} = \frac{R_s}{L_\sigma}\frac{m_r}{m_\mu}\sin\delta - \frac{m_u}{m_\mu}\frac{U_d}{U_d^*}\sin\delta_{u\mu} + \omega_u \tag{10}$$

$$\dot{\delta} = -\left(\frac{R_s}{L_\sigma}\frac{m_r}{m_\mu}+\frac{1}{T_\sigma}\frac{m_\mu}{m_r}\right)\sin\delta + \frac{m_u}{m_\mu}\frac{U_d}{U_d^*}\sin\delta_{u\mu} - p\omega_m \tag{11}$$

where

$$\delta_{u\mu}(t) = \chi_u(t) - \chi_\mu(t), \quad \delta(t) = \chi_\mu(t) - \chi_r(t). \tag{12}$$

The linearized model will be denoted by

$$y(t) = Gu(t) + G_d d(t) \tag{13}$$

where $y(t) = (T(t)\ m_\mu(t))^T$ and $d(t) = (U_d(t)\ \omega_\mu(t))^T$. The controllability analysis will be performed at zero torque and at nominal flux at three different stator frequencies, namely *10%* (OP1), *50%* (OP2) and *90%* (OP3) of base speed ω_0.

From (5) and (8)-(11) it now follows that at an operating point with torque, stator flux and mechanical rotor speed specified by T^*, m_μ^* and ω_m^*, the stationary states are given by

$$x^* = \begin{pmatrix} m_\mu^* \\ m_r^* \\ \delta_{u\mu}^* \\ \delta^* \end{pmatrix} = \begin{pmatrix} m_\mu^* \\ m_\mu^*\cos\delta^* \\ \arctan\left(\dfrac{\omega_u^* + \dfrac{R_s}{L_\sigma}\sin\delta^*\cos\delta^*}{R_s\left(\dfrac{1}{L_\mu}+\dfrac{1}{L_\sigma}\sin^2\delta^*\right)}\right) \\ \dfrac{1}{2}\arcsin\left(\dfrac{4}{3}\dfrac{L_\sigma}{p m_\mu^{*2}}T^*\right) \end{pmatrix} \tag{14}$$

and the stationary inputs by

$$u^* = \begin{pmatrix} m_u^* \\ \omega_u^* \end{pmatrix} = \begin{pmatrix} \dfrac{m_\mu^* R_s}{\cos\delta_{u\mu}^*}\left(\dfrac{1}{L_\mu}+\dfrac{1}{L_\sigma}\sin^2\delta^*\right) \\ p\omega_m^* + \dfrac{1}{T_\sigma}\tan\delta^* \end{pmatrix} \tag{15}$$

V POLES AND ZEROS

The poles and zeros of the linear process models at the three operating points are shown in Figure 2. The system is stable at all operating points with one LHP-zero and four LHP-poles. As the stator frequency increases, two poles approach the zero whereas the remaining two poles move along the imaginary axis with the stator frequency. Consequently the system gets less damped with increasing rotor speed. The smaller the stator resistance the closer the poles get to the imaginary axis.

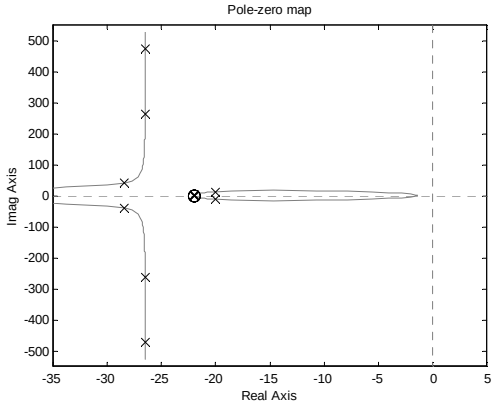

Figure 2: Pole-zero map of the induction machine.

VI TIME DELAYS

To represent a realistic controlled drive, a time delay should be added at the system input. Assuming that the time delay, T_d, is equal in all directions, the control bandwidth ω_B is limited by $\omega_B < 1/T_d$ [3].

VII RELATIVE GAIN ARRAY (RGA)

The relative gain array (RGA) is an indicator of sensitivity to uncertainty. Large RGA elements mean poor robustness for inverse based controllers in presence of independent input uncertainty [3], inevitable in practice. On the other hand, large RGA elements also mean that there is strong coupling and a diagonal controller is not likely to work satisfactory. By large is meant values above 10 [3]. The maximum RGA elements for the three operating points are plotted in Figure 3 as solid, dashed and dotted lines. As seen, there are peaks in the RGA elements corresponding to the

operating point stator frequency and the heights increase with the stator frequency. Most problematic are large RGA elements around the desired bandwidth. One possibility to avoid potential problems is to set the bandwidth above the operating point stator frequency, where the RGA-elements are small. Due to bandwidth constraints for example due to time delays, this may not be possible for higher stator frequencies and the RGA indicator limits the achievable bandwidth for those operating points. With a bandwidth independent of the operating point, it follows that it probably has to be less than the stator frequency at OP3.

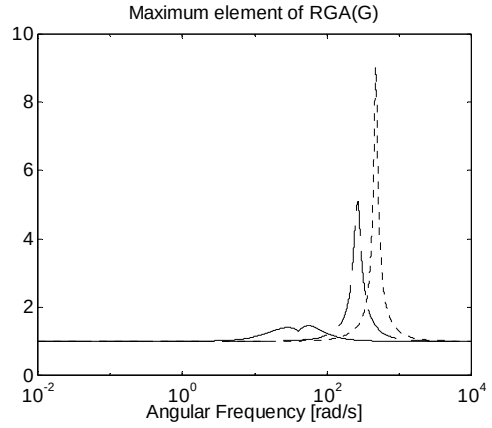

Figure 3: Maximum RGA elements.

Many control algorithms aim at decoupling the control of torque and flux, for example the classical field-oriented controller. Such controllers are inverse based and consequently are restricted to the limitations given by the RGA analysis above.

VIII SCALING

To easily examine performance requirements and limitations caused by input constraints, the system should be scaled. Introducing diagonal scaling matrices with the maximum expected values of the signals along the diagonals, the transfer functions change to

$$G = D_e^{-1}\hat{G}D_u, \quad G_d = D_e^{-1}\hat{G}_d D_d \tag{16}$$

where the original transfer functions are denoted with hats. Note that in the scaled representation the input constraints become $|u_i(t)| \leq 1$ and the and performance requirements become $|e_i(t)| \leq 1$, where the control error, $e(t)$, is the difference between a reference $r(t)$ and the output, $y(t)$. The limit on the stator voltage magnitude follows from (6) and although (7) only was set as a steady state restriction on the stator voltage frequency, it will used to scale this quantity. Hence, choosing the smallest deviation of the asymmetric limits we get

$$u_{1\max} = \min\left\{\frac{2}{\pi}U_d^* - m_u^*, m_u^*\right\}, \quad u_{2\max} = \frac{1}{T_\sigma} - \left|\omega_{slip}^*\right| \tag{17}$$

We require the control errors to be less than *5%* of rated torque and flux (see the appendix) and assume that the maximum disturbances on the inputs are *20%* of nominal DC-link voltage and *50%* of the pull-out slip frequency, respectively. Reference values are scaled as $r = R\tilde{r}$, where $R=D_e^{-1}D_r$ and the new input is upper limited by one. The matrix D_r defines the maximum expected reference changes, which we set to *100%* of rated torque and *10%* of rated flux.

IX SINGULAR VALUES

The largest and smallest singular values show the highest and lowest gains of the system over all directions. Small singular values mean that large inputs are needed in the corresponding input direction to effect the output and this might of course be a problem since there are constraints on the inputs. If for example disturbances or references act in the low gain output direction we might be in trouble. In Figure 4 the maximum and minimum singular values at OP2 are shown as solid lines. The maximum singular values show resonance peaks at the operating point stator frequencies, which could be expected from the pole-zero map in Figure 2. The minimum singular values on the other hand are smooth but decrease with the operating point stator frequency.

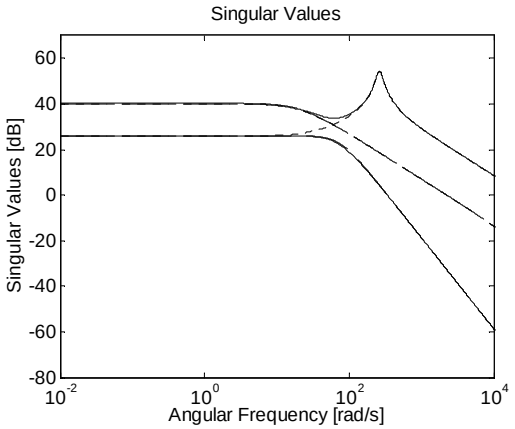

Figure 4: Singular values of the induction machine at OP2.

The dashed lines in the figure show the gains in the output torque and flux directions, i.e.

$$\left\| G(j\omega)\frac{G^{-1}(j\omega)y}{\left\|G^{-1}(j\omega)y\right\|_2}\right\|_2 = \frac{\|y\|_2}{\left\|G^{-1}(j\omega)y\right\|_2} \tag{18}$$

where y is set to $(1\ 0)^T$ and $(0\ 1)^T$, respectively. Finally, the dotted lines show the gains in the disturbance directions, i.e. plotting (18) with the columns of G_d instead of y. We see that the gain in the output flux direction follows the minimum singular values. This means that flux control requires large inputs. The gain in the output torque direction is higher although not the

maximum gain. It also turns out that the gain in the direction of the rotor speed disturbance coincides with the gain in the output torque direction and, at least for frequencies around and above the resonance, the gain in the direction of the DC-link voltage disturbance is very high. Hence the chances to suppress disturbances without violating input constraints do not seem too bad.

Although the condition number, the ratio between the largest and smallest singular values is large at many frequencies, the RGA, which is independent of scaling, indicated robustness problems only around the resonance frequencies.

A. *Flux Control Robustness*

As an example to illustrate the robustness issues discussed in connection to the RGA analysis, consider pure flux control at OP2. With the present scaling, the input direction for pure flux control at the resonance frequency is given by $(0.08\ 0.997e^{-i0.1})^T$, which is the input direction giving minimum gain. Now, the gain of the system in this direction is *4dB* compared to the gain in the input direction $(0\ 1)^T$, which is *33dB*. Hence a very small error in the input direction of pure flux control at the resonance causes large errors. The critical component is the error in amplitude, which corresponds to only *19 V*.

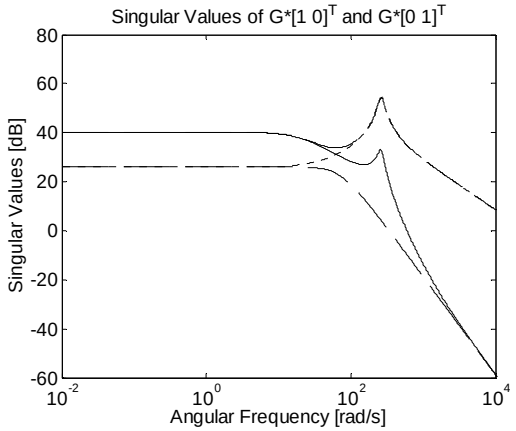

Figure 5: Gains in the stator voltage magnitude and frequency directions.

The issue is also visible in Figure 5, where the gains in the input directions $(1\ 0)^T$ (dotted line) and $(0\ 1)^T$ (solid line) are shown together with the maximum and minimum singular values (dashed lines). At the resonance frequency, the gain in the input direction $(0\ 1)^T$ is seen to be much larger than the minimum gain, corresponding to pure flux control. We also see that the stator voltage magnitude acts in the direction with minimum gain and the stator voltage frequency in the direction giving maximum gain for low frequencies. For high frequencies the situation is the opposite.

X LIMITATIONS IMPOSED BY INPUT CONSTRAINTS

Consider perfect control, i.e. *u(t)* is chosen as

$$u(t) = G^{-1}R\tilde{r}(t) - G^{-1}G_d d(t) \tag{19}$$

which gives $e(t) = 0$. The question asked is if selecting *u(t)* this way still satisfies the input constraint $|u| \le 1$. As the constraint on the stator voltage frequency may not be valid for transients, we will also consider the modified input constraint $|u_1| \le 1$. In the following two subsections, limitations caused by the input constraints are separately examined for disturbances and references.

A. *Disturbance Rejection*

If only disturbance rejection is considered, it follows that the available inputs are sufficient to perfectly cancel the effects of the disturbances if the following condition is met

$$\bar{\sigma}\left(HG^{-1}(j\omega)G_d(j\omega)\right) < 1 \tag{20}$$

where H is the identity matrix in case of the input constraint $|u| \le 1$ and the vector $(1\ 0)$ in case of $|u_1| \le 1$. Examining one disturbance at the time we replace G_d in (20) by its columns. As the DC-link disturbance actually adds to the stator voltage magnitude, which follows from equation (1), it turns out that (20) is satisfied as long as (if we use $m_u^* \approx m_\mu^* \omega_\mu^*$)

$$\omega_\mu^* \le \frac{2}{\pi} \frac{U_d^*}{1.2 m_\mu^*} \tag{21}$$

Relation (21) is satisfied with equality for $\omega_\mu = 440$ *rad/s*, which means that the DC-link voltage disturbance can not be completely rejected at OP3.

For rotor speed disturbances it turns out that even with the maybe too conservative constraint $|u| \le 1$, disturbances can be rejected for frequencies up to *1500 rad/s*, which is sufficient, as rotor speed disturbances usually are low frequency disturbances.

B. *Reference Tracking*

To perfectly track reference changes without violating the input constraints, we need the following condition to hold

$$\bar{\sigma}\left(HG^{-1}(j\omega)R(j\omega)\right) < 1 \quad , \forall \omega \le \omega_r \tag{22}$$

where ω_r is the frequency up to which reference tracking is required and the constant matrix H is defined as in the previous section. Now, if bandwidth is actually only required for torque control, one should study the inputs required by the torque reference alone and similarly for pure flux control. This means replacing the matrix R in (22) by its columns. From Figure 4 it is clear that flux control requires larger inputs than torque control. It follows that with the constraint $|u| \le 1$ and with reference step heights of *100%* of rated torque and *10%* of rated flux, the frequencies where the inputs

reach their limits for pure torque control become *16 Hz*, *18 Hz* and *17 Hz* at the three operating points. The corresponding values for flux control are *17 Hz*, *38 Hz* and *36 Hz*. If we instead consider the constraint $|u_1| \le 1$, the maximum torque bandwidths increase to *43 Hz*, *216 Hz* and *44 Hz*, whereas the bandwidth for flux control becomes unconstrained. This result can partly be understood from Figure 5. If the restriction on the stator voltage frequency is made weaker the solid line in Figure 5 is simply shifted upwards (together with the maximum and minimum gains). The gain in the output torque direction turns out to be upper bounded by the gain in the input direction $(1\ 0)^T$ and the torque control bandwidth is consequently upper bounded by the stator voltage magnitude constraint. The flux control bandwidth however increases with the limit on the stator voltage frequency.

XI PERFORMANCE CONSTRAINTS IMPOSED BY DISTURBANCES

Assume that the disturbances are cancelled with feedforward compensation as in (19). In a real control system there are always time delays and the feedforward compensation does not completely remove the influence of the disturbance but only reduces it from $G_d d$ to $G_d(1-e^{-sTd})d$, where T_d is the time delay. Hence, the best we can do with linear feedback is (here s denotes derivative)

$$e(t) = -Sr(t) + SG_d\left(1-e^{-sT_d}\right)d(t) \qquad (23)$$

where S is the sensitivity function. Considering one disturbance at the time, we get requirements on the sensitivity function in the directions where the disturbances act. The performance requirement is to keep the control error less than one and in order to reject disturbances the following relation must be fulfilled, where $G_{d\bullet i}$ denotes the i'th column of G_d

$$\max_{\omega} \left\| S(j\omega) G_{d\bullet i}(j\omega)\left(1-e^{-j\omega T_d}\right)\right\|_2 < 1, \quad i = 1,2 \qquad (24)$$

Hence we at least need

$$\underline{\sigma}\left(S(j\omega)\right) < \frac{1}{\left\|G_{d\bullet i}(j\omega)\right\|_2 \left|1-e^{-j\omega T_d}\right|} \quad ,\forall \omega, i \qquad (25)$$

The limit (25) for all three operating points are shown in Figure 6 as solid curves for the DC-link voltage disturbance and as dotted curves for the rotor speed disturbance at the three operating points. The time delay, T_d, is set to 1.5 times the sampling time, T_s, which is assumed to be *0.5 ms*. To satisfy the performance requirements, a very large bandwidth is required to suppress the DC-link voltage disturbance. As the bandwidths are limited by robustness and input constraints, we conclude that the performance requirements as stated above can not be satisfied, at least not for high rotor speeds.

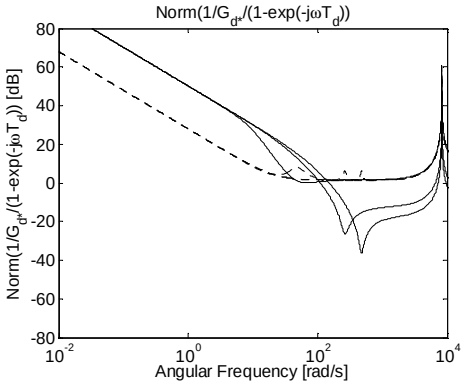

Figure 6: Performance constraint due to disturbances.

XII SIMULATIONS

This section shows simulation results to verify some of the theoretical results obtained through the controllability analysis. Throughout the simulations the Indirect Self Controller (ISC) described in [7] and [8] is used. This is a stator flux oriented controller aiming at decoupling the control of flux and torque. All simulation results are presented in the scaled representation defined by (16).

A. Consequences of Large RGA Elements

The analysis of the RGA elements indicated poor robustness for inverse based controllers. In [9] it was shown that ideally the ISC perfectly decouples the control of torque and stator flux at zero torque.

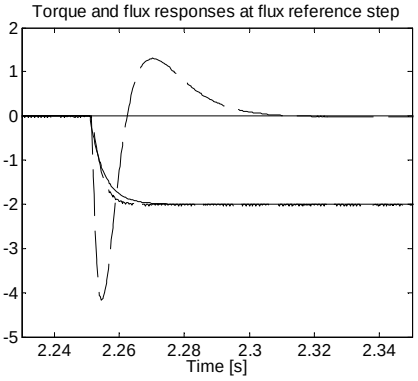

Figure 7: Responses to a flux step.

In Figure 7, the responses in torque and flux due to a step in the flux reference are shown for the ideal case with no time delays (solid lines) and with a realistic controller with a sample time of *0.5 ms* (dashed lines) at OP2. The controllers are tuned to give bandwidths of *40 Hz* with phase margins of 45° according to the tuning rules given in [9]. Note that the controller bandwidths coincides with the frequency where the RGA elements are large. The reference flux jumps from *100%* to *90%* of Ψ_0 at time *2.25s*. The ideal controller produces a flux

step with no disturbance on torque whereas the realistic controller with time delays generates large torque errors.

B. Disturbance Rejection

The investigation on disturbance rejection showed that suppression of DC-link voltages is limited by input- as well as bandwidth constraints whereas rotor speed disturbances should not be a problem. These results have been tested with the Indirect Self Controller, which basically does disturbance rejection according to (19).

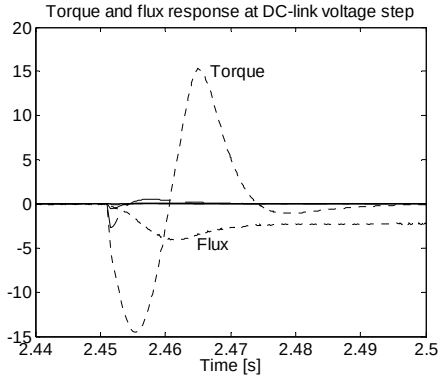

Figure 8: Control errors due to DC-link voltage step.

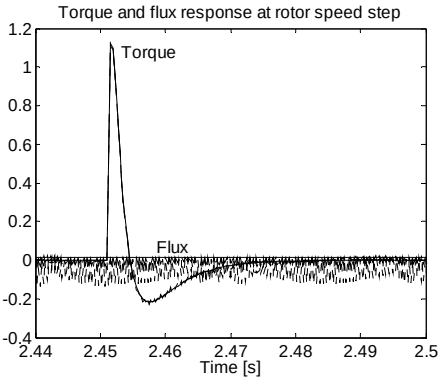

Figure 9: Control errors due to rotor speed step.

The sampling time was set to *0.5 ms* and the controllers were tuned to give maximum bandwidth with 45^{o} phase margin according to [9], i.e. *80 Hz* for torque control and *160 Hz* for flux control. Figure 8 shows the responses in torque and flux at a jump in the DC-link voltage from *750V* to *600V*. The responses at OP1 are shown as the solid lines, the responses at OP2 are shown as the dashed lines and finally the responses at OP3 are shown as the dotted lines. As seen the torque control error is large at OP3. It also follows that the stator voltage magnitude saturates, as the controller is not able to keep the flux at its reference value. Hence, both the input constraints as well as the performance constraints are violated as predicted above. High frequency components of the stator voltage magnitude, caused by the DC-link voltage mainly effect the torque whereas low frequency components effect the flux, c.f. Figure 5. The responses in torque and flux at a rotor speed disturbances of half the pull-out slip frequency are shown in Figure 9 for the three operating points. Just as predicted, this disturbance can be suppressed.

XIII CONCLUSIONS

The controllability analysis of the inverter fed induction machine among other things showed that the process has large RGA elements for large operating point stator frequencies, which causes problems with cross-coupling at flux control. If possible the controller bandwidths should be set higher than the operating point stator frequency to avoid problems. This may not be possible for higher stator frequencies due to for example long time delays. In this case at least the change rate of the flux reference should be limited to avoid exciting the critical frequencies around the operating point stator frequency. It was also shown that the DC-link voltage disturbance enters the system in a direction giving large gain around the resonance frequency. Due to input constraints and limited control bandwidth it cannot be completely suppressed for high stator frequencies.

XIV APPENDIX: Γ–MODEL MOTOR DATA

Stator resistance	R_s	=	18.5mΩ
Rotor resistance	R_r	=	17.3mΩ
Stator inductance	L_μ	=	6.2mH
Leakage inductance	L_σ	=	0.79mH
Number of pole pairs	p	=	2
Rated DC-link voltage	U_0	=	750V
Base speed	ω_0	=	528rad/s
Rated flux	Ψ_0	=	0.9Vs
Rated torque	T_0	=	600Nm

XV REFERENCES

[1] B. K. Bose, "High Performance Control and Estimation in AC Drives", *in 23rd International Conference on Industrial Electronics, Control and Instrumentation*, Volume: 2, 9-14, 1997.

[2] J. A. Santisteban and R. M. Stephan, "Vector Control Methods for Induction Machines: An Overview", *IEEE Transactions on Education*, 2001.

[3] S. Skogestad and I. Postlethwaite, *Multivariable Feedback Control*, John Wiley & Sons, 1996.

[4] L. Harnefors, On Analysis, *Control and Estimation of Variable-Speed Drives*, Ph D thesis, KTH, Stockholm, 1997.

[5] A. Steimel, "Stator-Flux-Oriented High Performance Control in Traction", *in 35th Annual Meeting IEEE IAS Industry Applications Society*. Rome, 2000.

[6] K. P. Kovacs, *Transient Phenomena in Electrical Machines*, Elsevier, 1984.

[7] M. Jänecke, R. Kremer, G. Steuerwald, "Direct Self Control, A Novel Method Of Controlling Asynchronous Machines In Traction Applications", *in Record of the EPE-Conference*, Aachen, 1989.

[8] D. Maischak, *Schnelle Drehmomentregelung im gesamten Drehzahlbereich eines hochausgenutzten Drehfeldantriebs*, VDI Verlag, 1995.

[9] H. Mosskull, "Tuning of Field-Oriented Controller for Induction Machines", *in IEE-PEMD*, Bath UK, 2002.